Optics Communications 282 (2009) 1406–1411

Contents lists available at ScienceDirect

Optics Communications

journal homepage: www.elsevier.com/locate/optcom

Double quasi phase matching for both optical parametric oscillator and difference frequency generation

Wei Quan Zhang *, Fan Yang, XiaoYun Li

Department of Physic Zhejiang Sci-Tex University, Key Laboratory of Advanced Textile Materials, Manufacturing Technology Ministry of Education, Hanghou, Zhjiang 310033, PR China

ARTICLE INFO

Article history:
Received 12 October 2007
Received in revised form 3 December 2008
Accepted 4 December 2008

Keywords:
Double phase matching
Phase matching bandwidth
Midwave infrared tune

ABSTRACT

We present simultaneous phase matching of optical parametric oscillator (OPO) and difference frequency generation (DFG), using a noncollinear interaction in periodically poled crystal with single grating. Selecting proper grating period Λ and titled angle ξ between the grating vector **G** and the optical axis of crystal, the noncollinear scheme provides double phase matching solutions over continuous regions of the midwave infrared spectrum. At certain wavelength regions, for DFG process the group velocities between interaction pulses are matching and the phase matching bandwidth reaches maximum. Selecting the different grating period, the broadband midwave tuning and better gain spectrum can be obtained at different wavelength range. For the certain period grating the conversion efficiency is higher. Hence, using the double phase matching configuration, the broadband tunable midwave infrared wave can be produced in single grating. But the configurations have a relatively narrow angular bandwidth.

1. Introduction

Using a resonant cavity and a single periodically poled crystal the midwave infrared (MWIR) sources is generated by both an optical parametric oscillator and difference frequency generation [1]. This simple configuration solved the high threshold problem but prevented tunability because of the unique phase matching conditions that had to be met for the OPO and the DFG processes to occur within the single poled crystal at a same temperature. To achieve tunable output, two separate periodically poled crystals were used within the resonator to allow for independent temperature phase matching of the two nonlinear processes [2–5]. In some cases, several nonlinear interaction should be phase-matched, e.g. for multiple optical parametric processes, all optical cascading effects, etc. [6,7]. Periodic structure has been used previously for simultaneous generation of several nonlinear processes in a collinear interaction [8,9], by relying on coincidence occurrence of two phase matching conditions at integer multiples of $2\pi/\Lambda$, where Λ is the QPM period. But this method is useful for a limited set of discrete wavelengths that satisfy this condition. Hence, it cannot generate tunable midwave infrared wave.

For frequency conversion of pulses, the phase matching bandwidth of pulse is limited by the group velocity (GV) mismatch. To increase conversion efficiency and decrease pulse distortions, it is significant to have simultaneous quasi phase matching (QPM) and GV matching in a nonlinear interaction process. If a spectral angular dispersion is introduced in the nonlinear interaction process, the achromatic phase matching technique can reach simultaneous QPM and GV matching. Schober et al. [10] have discussed GV-matched second harmonic generation. Zhang discussed group velocity matching OPO [11]. A noncollinear interaction can provide another degree of freedom that can be used, together with the QPM period, for phase matching simultaneously two different interactions. Furthermore, in a noncollinear configuration, the double phase matching (DPM) condition can be satisfied over a broad spectral range [12].

The purpose of this work is to explore the possibility of simultaneous GV matching and DPM in 1D poled crystal. It can generate a broadband tunable midwave infrared pulse by single periodically poled crystal. This paper is organized as follows: Firstly, noncollinear double quasi phase matching scheme for simultaneous OPO and DFG processes is presented. The phase matching equations are given. Second, the equations are applied to periodically poled KTP (PPKTP), and the tuning curve, phase matching bandwidth, gain spectrum and acceptance angles are discussed at DPM condition. Finally, we discuss the walk-off angle and effective nonlinear coefficient. Selecting different grating period of poled crystals, different tunable range of broadband midwave infrared pulse can be obtained.

2. Double quasi phase matching for both OPO and DFG processes

The Fig. 1 shows the vector scheme for noncollinear double quasi phase matching of OPO and DFG processes. In Fig. 1 $\mathbf{K_p}$, $\mathbf{K_s}$ and $\mathbf{K_i}$

* Corresponding author.
E-mail address: mike@hosonic.com.cn (W.Q. Zhang).

0030-4018/$ - see front matter © 2009 Elsevier B.V. All rights reserved.
doi:10.1016/j.optcom.2008.12.010

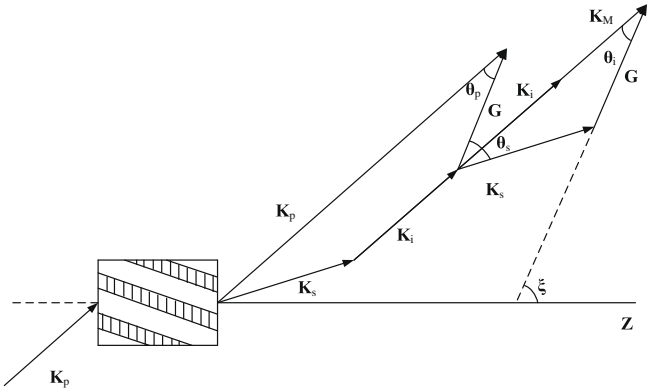

Fig. 1. Noncollinear double quasi phase matching scheme for both OPO and DFG processes.

denote the wave vectors of the pump, signal and idler waves, respectively, where $K_j = 2\pi\ n_j/\lambda_j$ ($j = p,s,i$). For OPO process the pump wave, signal wave and idler wave propagate at angles θ_p, θ_s and θ_i, respectively, with respect to the grating vector **G**, where $G = 2\pi/\Lambda$. ξ angle denotes the angle between **G** and z axis. In order to find the configuration that satisfies both phase matching conditions, one has to solve a set of two vector equations for the two different processes in periodic grating with a period Λ. The parametric conversion efficiency is strongly dependent on the wave vector mismatch. In OPO process the phase mismatch is given by

$$\Delta\mathbf{K} = \mathbf{K_p} - \mathbf{K_s} - \mathbf{K_i} - \mathbf{G} \tag{1}$$

The component parallel to the grating vector **G** is

$$\Delta K_{||} = K_p\cos\theta_p - K_s\cos\theta_s - K_i\cos\theta_i - 2\pi/\Lambda \tag{2a}$$

The perpendicular component is

$$\Delta K_{\perp} = K_p\sin\theta_p - K_s\sin\theta_s - K_i\sin\theta_i \tag{2b}$$

At phase matching, given the noncollinear angles θ_p and θ_s of the pump and signal wave vectors, the noncollinear angle θ_i of the idler wave vector is

$$\theta_i = arctg\left[\frac{(K_P\sin\theta_p - K_s\sin\theta_s)}{(K_p\cos\theta_p - K_s\cos\theta_s - 2\pi/\Lambda)}\right] \tag{3}$$

The signal and idler waves are subsequently used to generate the midwave infrared wave through the DFG process in the same poled crystal. For the process the phase matching condition is expressed as

$$K_s^2 + (K_i + K_M)^2 - 2K_s(K_i + K_M)\cos(\theta_s - \theta_i) = G^2 \tag{4}$$

where $\mathbf{K_M}$ is the wave vector of midwave infrared wave. Its direction is along the $\mathbf{K_i}$ direction. The θ_s–θ_i angle is the spatial walk-off angle between the signal and idler (or midwave infrared) wave vectors. In the principal axis coordinates, the direction cosines of wave vector **k** are

$$k_x = \sin\theta\cos\varphi, k_y = \sin\theta\sin\varphi, \quad k_z = \cos\theta \tag{5}$$

where θ is the angle between the wave vector and the Z axis, φ is the angle between the projection of wave vector in the X–Y plane and the X axis. The refractive indices in the wave vector direction are [13]

$$n_{\pm} = \{[e + A \pm (b^2 - 2Bb + A^2)]/2\}^{-1/2} \tag{6}$$

The calculations of A, B, e and b are shown in Ref. [13]. The n_+ and n_- correspond to fast (F) or slow (S) lights, respectively. The major refractive indices of the crystal increase with frequency at normal dispersion. The frequency of the pump beam is the largest in all beams. Because for same frequency $n_+ < n_-$, to satisfy the phase matching condition the pump beam must be fast light. Because the signal wave of OPO process is the pump wave of DFG process, the signal wave must also be fast light. Hence, for OPO process the phase matching type must be FFS match, i.e. pump and signal are both fast lights, idler is slow light. For KTP crystal a Sellmeier and thermo-optic dispersion formulas are shown is in Ref. [14].

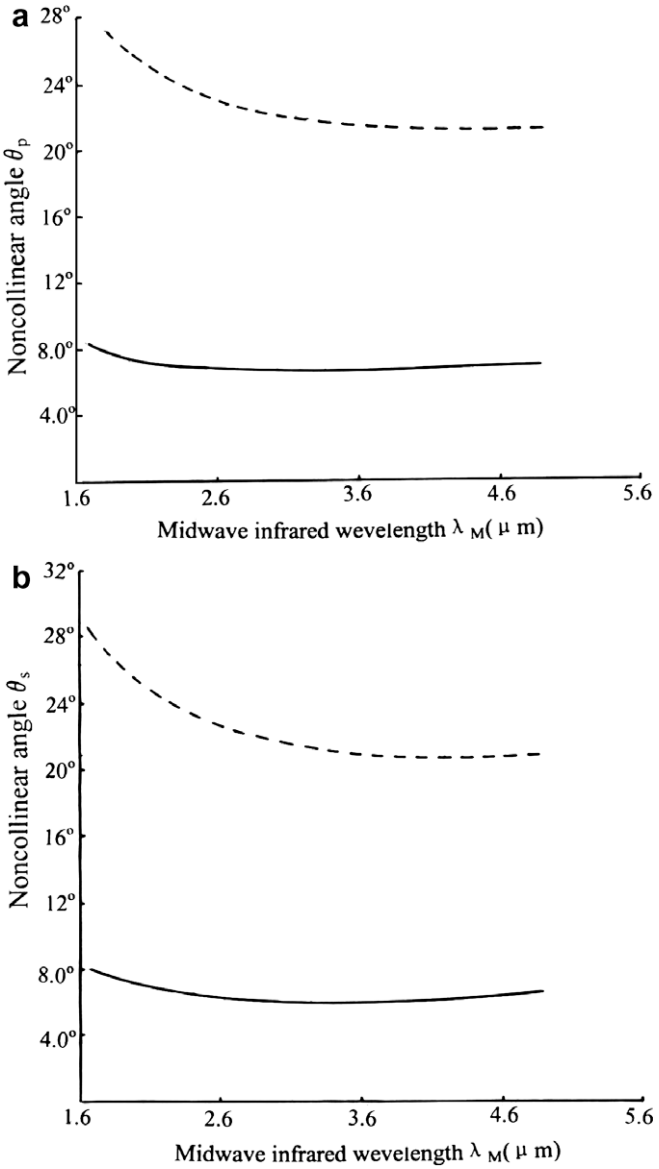

Fig. 2. Tuning curves: (a) angles θ_p as a function of midwave infrared wavelength λ_M; (b) angles θ_s as a functions of midwave infrared wavelengths λ_M at different grating period. Solid curve: Λ = 16.1 μm. Dashed curve: Λ = 13 μm.

The conditions of the energy conservation of the two processes are, respectively

$$\begin{aligned}\omega_p &= \omega_s + \omega_i \\ \omega_s &= \omega_i + \omega_M\end{aligned} \tag{7}$$

Given the wavelengths of pump and signal waves, that of idler and midwave infrared waves can be given. If the noncollinear angles θ_p, θ_s are changed, the phase matching condition Eq. (1) for OPO process can be met at a certain range of signal (idler) frequen-

cies. The OPO signal and idler waves are subsequently used to generate the MWIR wavelength though the DFG process.

Selecting proper titled angle ξ and grating period Λ, the phase matching condition Eq. (4) for DFG process can also be satisfied. At the time, double quasi phase matching conditions may be reached for both OPO and DFG processes in single poled crystal. Using the single periodically poled crystal, the midwave infrared tuning is realized. If the pump wavelength is 526 nm, the tuning curves are plotted as a function of midwave infrared wavelength in Fig. 2.

The two tuning curves correspond to values of two normalized grating periods. The solid curves correspond to Λ = 16.1 μm. The dashed curves correspond to Λ = 13 μm. Because any possible broad gain bandwidth only occurs around the position where the slopes of curves are zero nearly [15], from the Fig. 2 the broad gain bandwidth is produced when the phase matching noncollinear angle of signal light near 6.08° and that of idler (or MWIR) light is near 7.95° for Λ = 16.1 μm. The wavelengths were measured by an optical spectrum analyzer.

3. Group velocity matching and the phase matching bandwidth

The wave vector mismatching $\Delta K(\omega_0 + \Delta\omega)$ will be expanded in a Taylor series through second order:

$$\Delta K(\omega_0 + \Delta\omega) = \Delta K(\omega_0) + \frac{d[\Delta K(\omega)]}{d\omega}(\Delta\omega) + \frac{1}{2}\frac{d^2[\Delta K(\omega)]}{d\omega^2}(\Delta\omega)^2 \tag{8}$$

The phase matching condition is $\Delta K(\omega_0) = 0$. For DFG process, if the phase mismatch between wave vectors is ΔK, from Fig. 1, we obtain

$$(K_i + K_M - \Delta K)^2 = K_s^2 + G^2 + 2K_sG\cos\theta_s \tag{9}$$

Assume that the pump is monochromatic, $d\omega_p = 0$. We take the first-order derivative of both sides of the Eq. (9) with respect to ω_i, give

$$(K_i + K_M)\left(\frac{dK_i}{d\omega_i} + \frac{dK_M}{d\omega_i}\right) - (K_i + K_M)\frac{d\Delta K}{d\omega_i} = K_s\frac{dK_s}{d\omega_i} + G\cos\theta_s\frac{dK_s}{d\omega_i}$$

Hence $d\omega_s = -d\omega_i$ and $d\omega_M = -2\,d\omega_i$, give

$$\frac{d\Delta K}{d\omega_i} = \frac{dK_i}{d\omega_i} - 2\frac{dK_M}{d\omega_M} + \frac{dK_s}{d\omega_s}\frac{K_s + G\cos\theta_s}{K_i + K_M} \tag{10}$$

where $v_j^{-1} = d\,K_j/d\omega_j = (n_j - \lambda_j d\,n_j/\lambda_j)/c$ $(j = s,i,M)$. v_j^{-1} are called the group velocity. We take the derivative of the Eq. (10) with respect to ω_i, give

$$\frac{d^2\Delta K}{d\omega_i^2} = \frac{d^2K_i}{d\omega_i^2} + 4\frac{d^2K_M}{d\omega_M^2} + \frac{\left[(dK_i/d\omega_i - 2dK_M/d\omega_M)(dK_i/d\omega_i - 2dK_M/d\omega_M - d\Delta K/d\omega_i) - (K_s + G\cos\theta_s)\frac{d^2K_s}{d\omega_s^2} - \left(\frac{dK_s}{d\omega_s}\right)^2\right]}{K_i + K_M} \tag{11}$$

where $g_j = d^2K_j/d\omega_j^2 = (d^2n_j/d\lambda_j^2)\,\lambda_j^3/(2\pi c^2)(j = s,i,M)$. g_j are called the group velocity dispersion. Calculations of $d\,n_j/d\lambda_j$ and $d^2\,n_j/d\lambda_j^2$ are given in Ref. [16].

The relative parametric gain is

$$G_R = \mathrm{sinc}^2\{[(\Delta K/2)^2 - \Gamma^2]^{1/2}L\} \tag{12}$$

where L is an interaction length in the crystal and

$$\Gamma = 4\pi|E_s|d_{\mathrm{eff}}/(n_sn_i\lambda_in_M\lambda_M)^{1/2} \tag{13}$$

where d_{eff} (=$2/\pi d_{ij}$) is the effective nonlinear coefficient and E_s is the electric field intensity of the incident signal light (for DFG process it is the pump light). When $G_R = G_R^{\max}/2$, the corresponding phase mismatching is

$$\Delta K = 2[(1.392/L)^2 + \Gamma^2]^{1/2} \tag{14}$$

The phase matching bandwidth determined by the first-order term in Eq. (8) is

$$\Delta\lambda = \frac{2[(1.392/L)^2 + \Gamma^2]^{1/2}}{[d\Delta K(\lambda)/d\lambda|_{\lambda 0}]} \tag{15}$$

When the first order term is zero nearly, the bandwidth is determined by the second order term and

$$\Delta\lambda = \left\{\frac{4[(1.392/L)^2 + \Gamma^2]^{1/2}}{[d^2\Delta K(\lambda)/d\lambda^2|_{\lambda 0}]}\right\}^{1/2} \tag{16}$$

Because $|d\Delta K/d\omega_M| = 1/2|d\Delta K/d\omega_i|$, we can obtain the phase matching bandwidth $\Delta\lambda_M$ of midwave infrared pulse. Fig. 3 shows the phase matching bandwidth as a function of midwave infrared wavelength λ_M, where L = 10 mm and d_{ij} is calculated in Ref. [13]. In the Fig. the dashed curves correspond to $\Delta\lambda_M$ determined by the first order term. When the first order term is zero nearly, the phase matching bandwidth is determined by the second order term and the solid curves correspond to $\Delta\lambda_M$ determined by the second order term. Fig. 3a corresponds to Λ = 16.1 μm and Fig. 3b corresponds to Λ = 13 μm. When GV is matched, the phase matching bandwidths $\Delta\lambda_M$ determined by second order term are about 60 nm. The full-width half maximum (FWHM) $\Delta\lambda$ of the spectrum for 100 fs pulse is about 35 nm. The maximum effective interactive length $L_{\max}$ satisfies $L_{\max}\Delta\lambda = L\Delta\lambda_M$. At GV matching and $L = 1$ 0 mm, $L_{\max}$ = 17 mm and it is matching for the real length of crystal. We can also see that the phase matching bandwidth for Λ = 16.1 μm is larger than that for Λ = 13 μm. We note that their broadband tunable ranges are different. Hence, selecting different grating period, the different broadband tuning wavelength can be obtained.

The gain intensity is given [17] by

$$G = 1 + (\Gamma L)^2(\sinh B/B)^2 \tag{17}$$

where $B = (\Gamma - \Delta K/2)^{1/2}L$. The gain spectrums for some different noncollinear angles are shown in Fig. 4. When the noncollinear angles are 6.08° (Λ = 16.1 μm) or 21° (Λ = 13 μm) the gain spectrums are wider. From these results we know that the gain bandwidth is sensitive to noncollinear angle.

4. Acceptance angles

We consider the phase mismatching because noncollinear angles deviate from the idea noncollinear matching angles θ_p, θ_s. The phase mismatching ΔK is given by

$$\Delta K = \Delta K_0 + \frac{d\Delta K}{d\theta_h}(\Delta\theta_h) \quad (h = p,s) \tag{18}$$

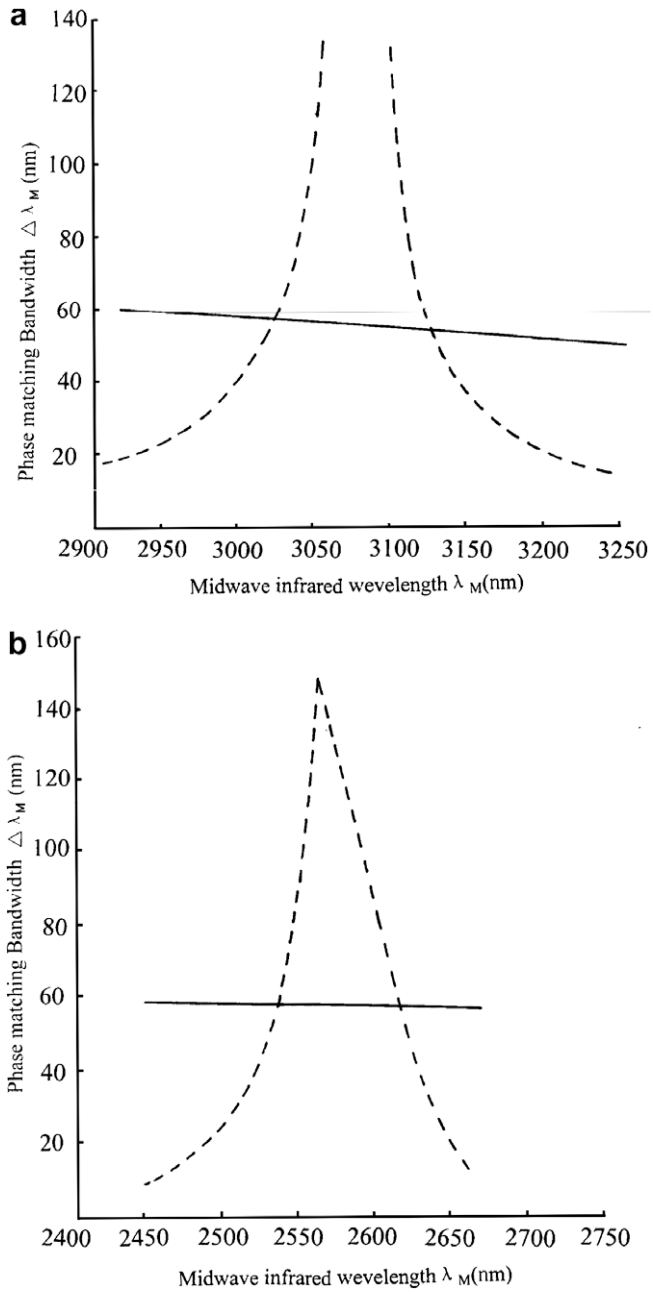

Fig. 3. Dependence of phase matching bandwidth $\Delta\lambda_M$ on midwave infrared wavelength λ_M. Solid curves: the $\Delta\lambda_M$ determined by the second order term. Dashed curves: the $\Delta\lambda_M$ determined by the first order term. (a) Λ = 16.1 μm; (b) Λ = 13 μm (crystal length L = 10 mm).

where $\Delta K_0 = 0$. For the first OPO process, we take the first order derivative of the Eq. (2a) with respect to θ_p, give

$$\frac{d\Delta K_{\parallel}}{d\theta_p} = \left(\frac{dK_P}{d\theta_p}\cos\theta_p - \frac{dK_i}{d\theta_p}\cos\theta_i\right) - \left(K_p\sin\theta_p - K_i\sin\theta_i\frac{d\theta_i}{d\theta_p}\right) \tag{19}$$

From Eq. (3), we obtain

$$\frac{d\theta_i}{d\theta_p} = \frac{K_p(\sin\theta_p tng\theta_i + \cos\theta_p) - dK_p/d\theta_p(\cos\theta_p tng\theta_i - \sin\theta_p)}{K_p\cos\theta_p - K_s\cos\theta_s - 2\pi/\Lambda} \times \cos^2\theta_i \tag{20}$$

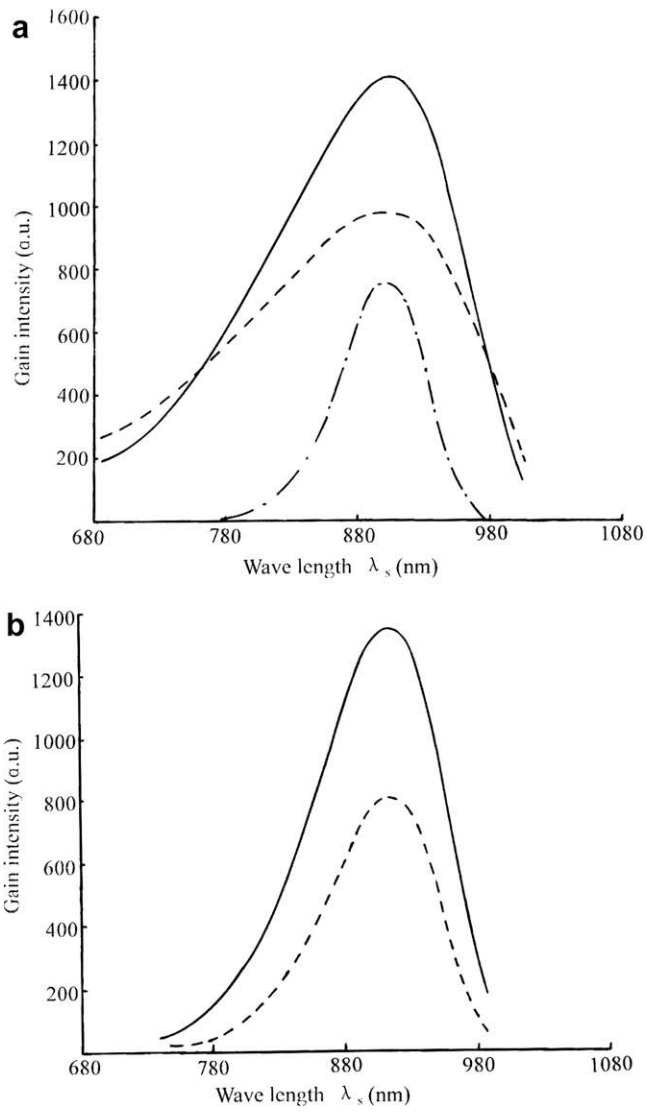

Fig. 4. In DPM condition the gain spectrum at given grating period Λ and corresponding noncollinear angle θ_s. (a) Solid curve: Λ = 16.1 μm, θ_s = 6.08°. Dashed curve: Λ = 16.05 μm, θ_s = 6.20°, spot-line curve: Λ = 16.02 μm, θ_s = 6.35°; (b) Solid curve: Λ = 13 μm, θ_s = 21°. Dashed curve: Λ = 13.03 μm, θ_s = 20.7°.

For the second DFG process, we take the first order derivative of both sides of the Eq. (9) with respect to θ_s, *give*

$$\frac{d\Delta K}{d\theta_s} = \frac{dK_i}{d\theta_s} + \frac{dK_M}{d\theta_s} - \frac{(K_s + G\cos\theta_s)dK_s/d\theta_s - K_sG\sin\theta_s}{K_i + K_M} \tag{21}$$

The calculations of $d\,K_j/d\theta_h$ are shown in Ref. [5] ($j = p, s, i$ or M, $h = p$ or s). From Eqs. (14) and (18), we can obtain the acceptance angles

$$\Delta\theta_h = \frac{2[(1.392/L)^2 + \Gamma^2]}{d\Delta K(\theta_h)/d\theta_h|_{h0}} \quad (h = p, s) \tag{22}$$

Fig. 5a and b show the dependences of the acceptances angles $\Delta\theta_s$ and $\Delta\theta_p$ on midwave infrared wavelength, respectively. The acceptance angles are that $\Delta\theta_s < 1.1°$ and $\Delta\theta_p < 0.2°$.

The acceptance angles for Λ = 13 μm are smaller than that for Λ = 16.1 μm. Note the angular tolerance for the double resonance phase matching is relatively tight. In experiment it is very important to keep the accurate noncollinear angle. The frequency angle tuning was a PPKTP crystal, held in a temperature controlled rotating stage with an angular resolution of 0.016°.

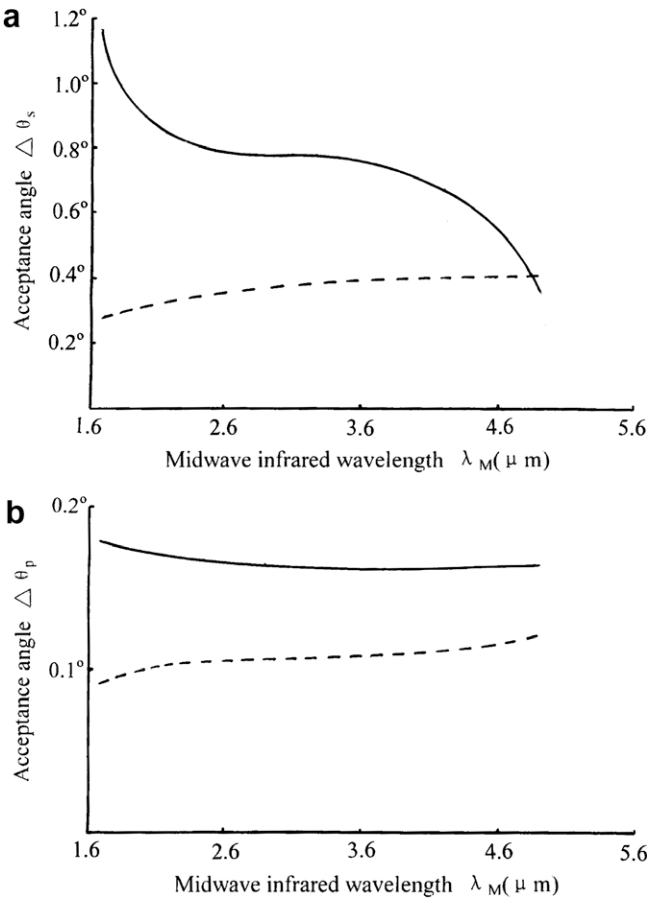

Fig. 5. (a) Dependence of acceptance angles $\Delta\theta_s$ on midwave infrared wavelength λ_M. (b) Dependence of acceptance angles $\Delta\theta_p$ on midwave infrared wavelength λ_M. Solid and dashed curves are the same as in Fig. 2.

5. Walk-off effect and effective nonlinear coefficient

The walk-off angle between the signal and midwave infrared Poynting vectors is

$$\theta_{\mathrm{MWIR,s}} = \cos^{-1}(S_{\mathrm{MWIR,x}}S_{\mathrm{sx}} + S_{\mathrm{MWIR,y}}S_{\mathrm{sy}} + S_{\mathrm{MWIR,z}}S_{\mathrm{sz}}) \tag{23}$$

where S_{ij} ($i = s$, MWIR and $j = x, y, z$) are the directions cosines of the signal and MWIR Poynting vectors, respectively. Their calculations are shown in Ref. [13]. Fig. 6 shows the dependence of the walk-off angle on midwave infrared wavelengths. The walk-off angle is smaller than 3°. The spatial walk-off that is due to noncollinear QPM and the walk-off of Poynting vectors may degrade the conversion efficiency. The walk-off length is described as $L_{a1} = D/ß$ and $L_{a2} = D/\theta_{\mathrm{MWIR,s}}$, respectively, where D is the beam width. Comparing Figs. 2 and 6, because walk-off angle $\theta_{\mathrm{MWIR,s}}$ of Poynting vectors is larger than the spatial walk-off angle $ß = \theta_p - \theta_s$, we regard the latter. For beam of 0.5 mm diameter, maximal interaction length L_{a2} = 10 mm .The length can match to the periodically poled crystal length. Although the noncollineary increases walk-off effect, but the walk-off does not affect interaction length.

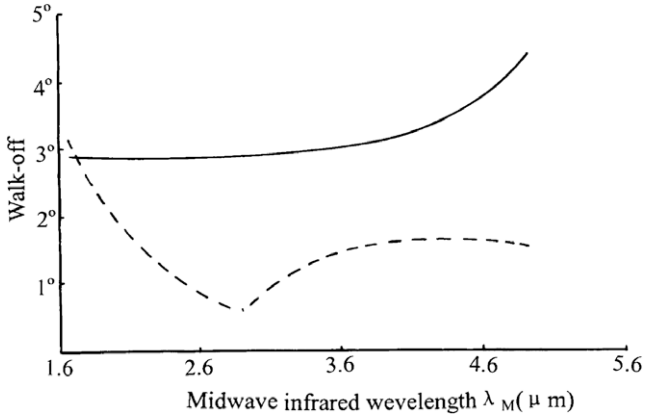

Fig. 6. Walk-off angles between Poynting vectors as a function of midwave infrared wavelength λ_M. Solid and dashed curves are the same as in Fig. 2.

The effective nonlinear coefficient is [13]

$$d_{\mathrm{eff}} = \alpha_i d_{ijk}\alpha_j\alpha_k \quad (i,j,k = x,y,z) \tag{24}$$

where $\alpha_i = k_i G/(1 - n_i^2/n^2)$ and $G = \left[\sum(k_i^2/(1 - n_i^2/n^2))^2\right]^{-1/2}$ ($i = x, y, z$). Fig. 7a and b show the results that correspond to Λ = 16.1 μm and Λ = 13 μm, respectively. In the figures solid curves correspond to DFG process, dashed curves correspond to OPO process. From the figures one can find that for Λ = 16.1 μm the effective nonlinear coefficient of DFG process is far larger than that of OPO process and for Λ = 13 μm they are near. Comparing Fig. 7a and b it can also find that the effective nonlinear coefficient of Λ = 13 μm is larger than that of Λ = 16.1 μm. The latter $d_{\mathrm{eff}}^{\max}$ is about 12.8 pm/v and it gets near d_{33} (13.7 pm/v). The conversion

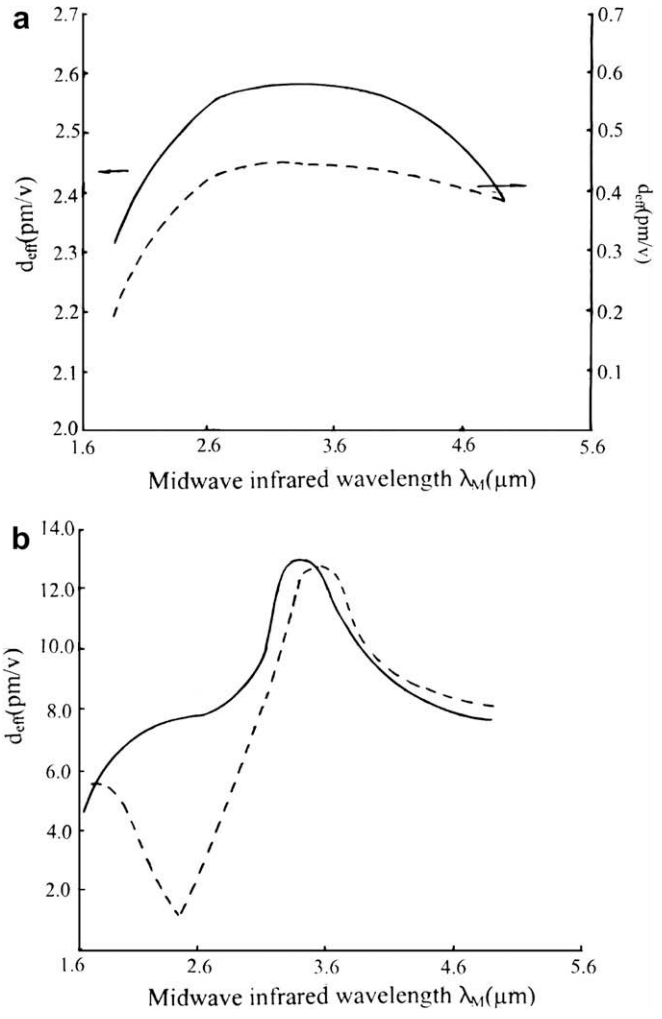

Fig. 7. Effective nonlinear coefficients d_{eff} as a function of midwave infrared wavelength λ_M; (a) for Λ = 16.1 μm, (b) for Λ = 13 μm. Solid curves correspond to DFG process, dashed curves correspond to OPO process.

efficiencies increase with effective nonlinear coefficient d_{eff}. For $\Lambda = 16.1$ μm because the d_{eff} of OPO process is very small, the conversion efficiencies for an OPO/DGF are smaller than that for direct generation of MWIR in an OPO. For $\Lambda = 13$ μm both effective nonlinear coefficients of OPO and that of DFG are larger, the conversion efficiencies are also larger.

6. Conclusion

We have given double quasi phase matching conditions for both OPO and DFG processes in the single periodically poled crystal. Selecting proper grating period, the midwave infrared tune from 1.6 μm to 4.9 μm can be realized. We calculate the acceptance angle. The acceptance angles $\Delta\theta_p$ and $\Delta\theta_s$ are about 0.2° and 0.8° for $\Lambda = 16.1$ μm, respectively. Note that the angular tolerance for the double resonance phase matching is relatively tight. We have also given the phase matching bandwidth. The phase matching bandwidth is primarily determined by the first order term in the expansion of wavevector mismatch. In most case, the first-order term is larger and consequently the phase matching bandwidth is small. If the first-order term vanishes, the phase matching bandwidth is determined by the second order term. This usually leads to greatly enhanced phase matching bandwidth. Selecting different grating period, different tunable range of broadband midwave infrared can be obtained. At the time the phase matching bandwidth of pulse is larger. The maximum effective interactive length will be enhanced. When the noncollinear tuning angle θ_s with respect to the grating vector are about 6.08° for $\Lambda = 16.1$ μm, or that are about 21° for $\Lambda = 13$ μm, broad gain bandwidth will occur. The broadband gain spectrum can be give. The maximum interaction length limited by walk-off effect can match to the periodically poled crystal length. Therefore, the single PPKTP can be used with noncollinear geometry for the broadband DPM with the tunable pulse. This analysis is adaptive to other QPM materials.

References

[1] D. Chen, K. Masters, Opt. Lett. 26 (2001) 25.
[2] Da Wun Chen, Opt. Soc. Am. B 20 (7) (2003) 1527.
[3] David Artigas, Derryck T. Reid, Opt. Commun. 210 (2003) 113.
[4] Karl A. Tillman, Derryck T. Reid, Opt. Am. B 21 (8) (2004) 1551.
[5] W.Q. Zhang, Opt. Commun. 252 (2005) 179.
[6] Stefano Longhi, Opt. Lett. 26 (10) (2001) 713.
[7] Chao-Kuei Les, Jing Yuan Zhang, J.Y. John Huang, Ci-Ling Pan, J. Opt. Soc. Am. B 21 (8) (2004) 1494.
[8] Yi-Qiang Qin, Yong-Yuan Zhu, Chao Zhang, Nai-Ben Ming, J. Opt. Soc. Am. B 20 (1) (2003) 73.
[9] Husam H. Abu-Safe, Appl. Opt. 44 (34) (2005) 7458.
[10] A.M. Schober, M. Charbonnaeun-Lefort, M.M. Fejer, J. Opt. Soc. Am. B 22 (2005) 1699.
[11] W.Q. Zhang, Appl. Opt. 45 (20) (2006) 4977.
[12] S.M. Saltiel, A.A. Sukhorukov, Y.S. Kivshar, Prog. Opt. 47 (2005) 1.
[13] W.Q. Zhang, Opt. Commun. 105 (1994) 226.
[14] K. Kato, E. Takaoka, Appl. Opt. 41 (2002) 5040.
[15] C. Wang, Y.X. Leng, et al., Opt. Commun. 273 (2004) 169.
[16] W.Q. Zhang, OPTIK (Stuttgart) 104 (1997) 87.
[17] J.A. Armstrong, N. Blormbegen, J. Ducuing, P.S. Rershan, Phys. Rev. 127 (1962) 1918.